SOLID STATE CONVECTION MODELS OF THE LUNAR INTERNAL TEMPERATURE

Gerald Schubert
Department of Geophysics and Space Physics
University of California
Los Angeles, California 90024

Richard E. Young and Patrick Cassen
NASA Ames Research Center
Moffett Field, California 94035

May 15, 1975

ABSTRACT

Thermal models of the Moon, which include cooling by subsolidus creep and consideration of the creep behavior of geologic material, provide estimates of 1500 to 1600 °K for the temperature, and 10^{21}-10^{22} cm^2/sec for the viscosity of the deep lunar interior.

INTRODUCTION

There is no question that the advection of temperature by the subsolidus creep of geologic material is an a-priori important mechanism of heat transport in the interiors of all the terrestrial planets. To what extent heat transfer by solid state convection dominates the thermo-mechanical state of a planet's interior depends on the rheological behavior of the material as a function of its temperature, pressure, stress, volatile content, etc., and, of course, on the values of these properties within the body. Although there are other uncertainties in the construction of thermal models of a planet, and we do not mean to downplay these difficulties, our lack of knowledge of the appropriate stress-rate of strain law to apply under conditions of very high pressure, in particular, is a major source of uncertainty in assessing the importance of solid state convection. In this connection, the question of whether convection is confined to the upper mantle of the Earth or extends throughout the entire mantle is one of much current debate.

In the case of the Moon, our knowledge of the rheological law governing subsolidus deformation is, at the moment, probably on firmer ground than for any of the other terrestrial planets save the upper mantle of the Earth. This is mainly because of the small size of the Moon; the pressure at the center of the

Moon is about equal to that at a depth of 150 km in the Earth. None of the major silicate phase transitions known to occur at depths of 400 and 650 km in the Earth can take place on the Moon. Thus we may use our rapidly expanding understanding of the rheological behavior of geologic materials characteristic of the Earth's upper mantle, obtained from post-glacial rebound studies and laboratory measurements of rock and single mineral crystal deformation, to model the creep behavior of the entire lunar interior. Of particular importance here, in view of the extensive depletion of volatiles in lunar material, is the recent determination of the law governing the low-stress, high-temperature creep in dry olivine single crystals by Kohlstedt and Goetze (1974).

The possible role of solid state convection in regulating the Moon's internal temperature has long been advocated by Runcorn (1962, 1967) on the basis of the departure of the lunar figure from hydrostatic equilibrium and by Tozer (1972) on the basis of the creep behavior of rocks at elevated temperatures. Linear stability analyses, including effects of variable viscosity, indicate that thermal conduction models of the Moon would likely be unstable against subsolidus convection (Schubert, Turcotte and Oxburgh 1969, Cassen and Reynolds 1973, 1974). Estimates of the viscosity of lunar material below several hundred kilometers depth (Meissner 1975) support the possibility of solid state convection beneath a relatively rigid lithosphere.

A numerical, finite-difference calculation of the lunar temperature including heat transport by solid state convective motions of finite amplitude (Turcotte, Hsui, Torrance and Oxburgh 1972) shows the substantial cooling and homogenizing effect of subsolidus creep. Convection model temperatures are much lower, and when averaged over a spherical surface, they are much more uniform with depth than temperatures computed on the basis of heat transfer by conduction alone. Cassen and Young (1975) have quantitatively investigated the role of finite-amplitude subsolidus convection in cooling and eventually solidifying a possible molten or partially molten lunar core. They found that solid state creep is such an efficient heat transport mechanism that if radioactive heat sources were completely removed from the lunar interior by differentiation, any molten core would rapidly solidify on a geologic time scale. However, if radioactives were present in the Moon's interior, these heat sources would supply the heat flux carried by subsolidus convection and temperatures sufficiently high for a molten or partially molten core would be maintained.

In this paper we numerically calculate lunar temperature profiles and their dependences on viscosity of the lunar interior for models which include finite-amplitude solid state convective cooling. Since the temperature in regions of subsolidus creep is relatively uniform with depth we can plot the deep lunar temperature as a function of viscosity; this

temperature increases with increasing viscosity since the more viscous the interior, the less vigorous the convection and the less efficient the cooling by solid state creep. In addition, our knowledge of the laws governing deformation of geologic materials likely to be representative of those inside the Moon enables us to calculate viscosity-temperature dependences. If we plot temperature against viscosity according to the rheological behavior of geologic material, we find temperature to decrease with increasing viscosity. The intersection of these two temperature vs. viscosity curves determines the thermal state of the lunar interior consistent with both solid state convection and the rheological behavior of geologic material. We find that the deep lunar temperature is between about 1500 and 1600 $^{\circ}$K with an effective viscosity between 10^{21} and 10^{22} cm^2/sec.

The Apollo program of lunar exploration has provided us with measurements of the seismic velocities and electrical conductivity of the Moon's interior, and the heat flux at two locations on the Moon's surface. These geophysical data can be used to infer characteristics of the lunar temperature profile. In the concluding section these data are discussed, and their implications for the Moon's temperature are compared with our thermal models.

DESCRIPTION OF THE MODEL

Our model of the Moon's interior consists of a rigid outer spherical shell, the lithosphere, surrounding a spherical shell, the mantle, in which subsolidus convection can occur. We allow for a small, central core following the speculation of Nakamura et al. (1974). Radioactive heat sources are assumed to be distributed uniformly throughout the lithosphere and mantle with a concentration Q (energy/time/volume). An arbitrary concentration of heat sources may exist very near the lunar surface as a result of previous differentiation without affecting the interior thermal state. A major assumption of our model is that sufficient heat sources have been retained in the interior to drive a convective flow. The mantle is taken to be a Boussinesq fluid with infinite Prandtl number, so that we neglect inertial terms in the equations of motion - a fully justifiable assumption for the highly viscous material of the lunar mantle.

The numerical calculations of subsolidus convection in the mantle are carried out for a mantle of constant kinematic viscosity ν. However, as discussed in the introduction, we investigate a range of values of viscosity and determine 'the' internal lunar temperature and viscosity as that set of values which simultaneously satisfy the convective thermal model calculations and the likely rheological law for deformation of

lunar material. The fact that the spherically-averaged lunar temperature is almost constant with depth allows the procedure to be meaningful.

Other physical properties pertinent to the thermal calculations, such as density ρ, thermal conductivity k, thermal expansivity α, and specific heat at constant pressure c_p are assumed to be constant and to have the same values for both the lithosphere and mantle.

The boundary conditions for the calculations are:

1) A constant temperature $T = T_s$ at the lunar surface $r = R_s$ (r is the radial location of a point in the Moon).
2) Continuity of temperature and heat flux at the mantle-lithosphere boundary $r = R_o$.
3) An insultaing core-mantle boundary, i.e. no heat leaves or enters the core at any place on the core-mantle interface $r = R_i$. With this boundary condition we need not place any a-priori specification on the deep lunar temperature. Further, if a small lunar metallic core did exist it would contain only a relatively unimportant quantity of K^{40} (Ganguly and Kennedy 1975) and supply an essentially negligible fraction of the surface lunar heat flux. Neither could the cooling and solidification of such a small core provide a non-negligible portion of the lunar heat flow for any substantial fraction of geologic time.

4) Free-rigid velocity boundary conditions for the convecting mantle. The core-mantle boundary would likely approximate a free boundary (i.e. zero tangential stress) if the core were liquid. The mantle-lithosphere boundary is most certainly a rigid one (i.e. the velocity of the convecting mantle must be zero at this interface) in light of both the apparent thickness of the lithosphere, at least several hundred kilometers, and the absence of any surface expression of horizontal displacements of parts of the lithosphere.

The equations and boundary conditions of the model are summarized in mathematical form as follows. Time t, distance $\underline{r}$, velocity $\underline{u}$, pressure p, and temperature T are assumed dimensionless with respect to $(R_o-R_i)^2/\kappa$, (R_o-R_i), $\kappa/(R_o-R_i)$, $\rho\nu\kappa/(R_o-R_i)^2$, and $Q(R_o-R_i)^2/k$, respectively, where κ is the thermal diffusivity $k/(\rho c_p)$. The temperature is referenced to the spherically symmetric conduction profile, i.e. in addition to being dimensionless, T is the difference between the temperature and the value of the spherically symmetric conduction temperature at the mantle-lithosphere interface.

The equations governing the temperature and velocity fields in the mantle are:

$$\nabla\cdot\underline{u} = 0 \quad , \qquad (1)$$

$$\frac{\partial T}{\partial t} + \underline{u}\cdot\nabla T = \nabla^2 T + 1 \quad , \qquad (2)$$

$$0 = -\nabla p + \nabla^2 \underline{u} + Ra\left(1 + \frac{S}{r^3}\right)\underline{r}T \quad , \qquad (3)$$

where

$$Ra = \frac{4\pi\alpha G\rho (R_o - R_i)^6}{3k\nu\kappa} \quad , \qquad (4)$$

$$S = \frac{R_i^3}{(R_o - R_i)^3}\left\{\left(\frac{R_s^3}{R_i^3} - 1\right)\left(\frac{M_c}{M - M_c}\right) - 1\right\} \quad , \qquad (5)$$

G is the gravitational constant, M is the total mass of the Moon and M_c is the mass of the central core. The Rayleigh number Ra is the parameter measuring the vigor of the convection and S is the parameter characterizing the variation in acceleration of gravity due to self-gravitation of the body.

The boundary conditions for equations (1)-(3) are

$$u_r = \frac{d^2}{dr^2}(ru_r) = \frac{dT_a}{dr} = \frac{dT_{\ell m}^{c,s}}{dr} = 0, \text{ on } r = \overline{\beta} - 1, \qquad (6)$$

$$\underline{u} = 0, \quad T_a = 0, \quad \text{on } r = \overline{\beta} \quad , \qquad (7)$$

$$T_{\ell m}^{c,s}/(dT_{\ell m}^{c,s}/dr) = \frac{(1 - \overline{\alpha}^{2\ell+1})\overline{\beta}}{\ell + (\ell+1)\overline{\alpha}^{2\ell+1}}, \quad \text{on } r = \overline{\beta} \quad , \qquad (8)$$

where

$$\overline{\alpha} = R_s/R_o, \quad \overline{\beta} = R_o/(R_o - R_i) \quad , \qquad (9)$$

and u_r is the radial component of velocity. In writing (6)-(9), we have considered the temperature as the sum of two parts, $T_a(r)$, the average value of T on a spherical

surface and an angular dependent part

$$\sum_{\ell=1}^{\infty} \sum_{m=0}^{\ell} P_{\ell m}(\cos\theta)\left\{T^{c}_{\ell m}(r)\cos m\varphi + T^{s}_{\ell m}(r)\sin m\varphi\right\} \quad , \qquad (10)$$

where r, θ, φ are spherical coordinates and $P_{\ell m}(\cos\theta)$ are the associated Lengendre functions.

Equation (8) follows from the continuity of temperature and heat flux at the mantle-lithosphere boundary and assumes that the lithospheric temperature is given as the solution of the steady state heat conduction equation. Thus this boundary condition is only an approximation for non-steady conditions. Finally we note that the dimensionless steady-state conduction temperature profile is

$$\frac{\bar{\beta}^2}{6} + \frac{(\bar{\beta}-1)^3}{3\bar{\beta}} - \frac{(\bar{\beta}-1)^3}{3r} - \frac{r^2}{6} \quad . \qquad (11)$$

A complete solution of the problem requires specification of the geometrical parameters $\bar{\alpha}$ and $\bar{\beta}$, the Rayleigh number Ra and the self-graviation parameter S.

VISCOSITY DEPENDENT SUBSOLIDUS CONVECTION TEMPERATURES

The equations governing the temperature and velocity field in the convecting mantle are solved numerically using the method of Young (1974), wherein velocity and temperature variables are expanded in surface spherical harmonics $P_{\ell m}(\cos\theta)$ $\binom{\sin m\varphi}{\cos m\varphi}$ with coefficients depending on r. We have investigated only the axisymmetric, m = 0, modes of convection in the mantle.

Model Parameter Values

In the previous section we noted that the state of thermal convection in the mantle depended only on the parameters Ra, S, $\bar{\alpha}$ and $\bar{\beta}$. To evaluate the latter two geometric quantities, we must choose values for the core radius R_i and the outer radius of the mantle R_o (R_s = 1740 km). The radius of a possible metallic core in the Moon is necessarily small because of the value of $C/(MR_s^2)$ (C is the moment of inertia about the rotation axis), 0.395±0.005 (Sjogren 1971, Williams et al. 1974, Kaula et al. 1974), which is very close to the value of 0.4 for a homogeneous Moon. The radius of a pure iron core is limited to 300-400 km; if the core contained a lighter alloying element the radius could be somewhat larger. We choose R_i = 300 km. The precise size of such a small

lunar core would not be expected to significantly influence the deep lunar temperature.

There is considerably more uncertainty in the choice of the thickness of the rigid lithosphere ($R_s - R_o$). This must be at least a few hundred kilometers to support the mascons (Arkani-Hamed 1973) and could conceivably be as thick as about 800 km (Nakamura et al. 1973). It is important to note that the lithosphere thickness must be chosen consistent with the assumed value of the concentration of heat producing radioactives Q, i.e. the temperature at the base of the lithosphere must not greatly exceed (or fall far below) that temperature at which geologic material can undergo significant subsolidus creep on a geologic time scale. Although the temperature at which creep becomes important cannot be precisely defined, we will see in our discussion of rheological behavior that it is probably about 1000 °C.

The steady state (dimensional) temperature at the base of the lithosphere, averaged over the spherical surface, is

$$T_s + \frac{Q(R_s^2 - R_o^2)}{6k} + \frac{QR_i^3}{3k}\left(\frac{1}{R_s} - \frac{1}{R_c}\right) \quad , \qquad (12)$$

where T_s is the surface temperature, $T = T_s$ at $r = R_s$. Using R_i = 300 km, R_s = 1740 km, $k = 4 \times 10^5$ erg/(cm sec °K) and T_s = 0 °C in expression (12), we can determine those values of Q and R_o that give reasonable temperatures (~1000 °C) at the base of the lithosphere. We have considered two models. In

the first, the lithosphere thickness is 300 km, R_o = 1440 km, $\bar{\alpha}$ = 1.208, $\bar{\beta}$ = 1.263, and S = 0.0258. This lithosphere thickness, together with a value of $Q = Q_\oplus = 2.6\times10^{-7}$ erg/(cm^3 sec) gives an average temperature of 1026.5 °C at the base of the lithosphere ($Q_\oplus$ is the terrestrial value of Q, obtained by assuming that the Earth's surface heat flow originates from radioactive sources uniformly distributed throughout the Earth's mantle). The second model has a lithosphere thickness of 800 km, R_o = 940 km, $\bar{\alpha}$ = 1.851, $\bar{\beta}$ = 1.459, S = 0.1460, $Q = Q_\oplus/2$ and an average lithosphere base temperature of 1150 °C.

Only the Rayleigh number remains to be discussed. With Q given as either $Q_\oplus$ or $\frac{1}{2}\,Q_\oplus$ and (R_o-R_i) having the corresponding values of 1140 km and 640 km, we can write Ra as

$$Ra = \frac{4\times10^{27}}{\nu(\text{cm}^2/\text{sec})} \quad \text{or} \quad \frac{6.3\times10^{25}}{\nu(\text{cm}^2/\text{sec})} \tag{13}$$

for the thin and thick lithosphere models, respectively. In arriving at these Ra-ν relations we have additionally assumed $\alpha = 3\times10^{-5}\ ^\circ\text{K}^{-1}$, $\rho = 3.34$ g/cm^3, $k = 4\times10^5$ erg cm^{-1} sec^{-1} $^\circ\text{K}^{-1}$ and $\kappa = 10^{-2}$ cm^2/sec.

For a thin or thick lithosphere model, we make a series of thermal convection calculations for Rayleigh numbers ranging from the critical value Ra_{crit} to as much as 500 Ra_{crit}. According to linear stability theory the mantle is static for $Ra<Ra_{crit}$ and the temperature is the steady state conduction temperature ; at $Ra>Ra_{crit}$ convection occurs. With increasing

Ra or decreasing viscosity ν, convection becomes more vigorous and efficient at cooling the mantle, and the deep lunar temperature decreases. Thus for the thin or thick lithosphere model we know the deep temperature of the Moon as a function of viscosity. To decide which temperature and viscosity characterize the real Moon we incorporate rheological information.

Linear Stability Calculations

The value of the critical Rayleigh number and the state of convection in the mantle at the onset of instability can be determined independently of the numerical finite-amplitude convection calculations. This is important because the separate stability computation provides both a check on the finite-amplitude method and a set of temperature and velocity variables with which to start the finite-amplitude computations. The equations and boundary conditions for the linearized stability problem are (see Chandrasekhar 1961)

$$\left(\frac{(\bar{\beta}-1)^3}{r^3} - 1\right)\frac{(ru_r)^{c,s}_{\ell m}}{3} = \left(\frac{d^2}{dr^2} + \frac{2}{r}\frac{d}{dr} - \frac{\ell(\ell+1)}{r^2}\right)T'^{c,s}_{\ell m} \quad , \quad (14)$$

$$\left(\frac{d^2}{dr^2} + \frac{2}{r}\frac{d}{dr} - \frac{\ell(\ell+1)}{r^2}\right)^2 (ru_r)^{c,s}_{\ell m} = Ra\left(1+\frac{S}{r^3}\right)\ell(\ell+1)T'^{c,s}_{\ell m}, \quad (15)$$

$$(ru_r)^{c,s}_{\ell m} = \frac{d^2}{dr^2}(ru_r)^{c,s}_{\ell m} = \frac{d}{dr}T'^{c,s}_{\ell m} = 0, \quad \text{on } r = \bar{\beta}-1 \quad , \quad (16)$$

$$(ru_r)^{c,s}_{\ell m} = \frac{d}{dr}(ru_r)^{c,s}_{\ell m} = 0 \quad \text{on } r = \bar{\beta} \quad , \quad (17)$$

$$T'^{c,s}_{\ell m}(\ell+(\ell+1)\bar{\alpha}^{2\ell+1}) = \frac{dT'^{c,s}_{\ell m}}{dr} - (1-\bar{\alpha}^{2\ell+1})\bar{\beta}, \quad \text{on } r = \bar{\beta} \quad , \quad (18)$$

where T' is the temperature perturbation (the amount by which the temperature exceeds the conduction temperature profile) and the $(^{c,s}_{\ell m})$ notation has been introduced in expression (10).

The linearized stability problem is actually independent of m. Since the system (14)-(18) is homogeneous it possesses a nontrivial solution only for certain values of Ra, i.e. Ra_{crit}, which for a given set of values of $\bar{\alpha}$, $\bar{\beta}$ and S, depend only on ℓ. Figure 1 shows these values of Ra_{crit} as functions of ℓ for the thin and thick lithosphere models and the free-rigid velocity boundary conditions. The critical Rayleigh numbers for the thin lithosphere model with free-free velocity boundary conditions are also shown for purposes of comparison. Although continuous curves connect values of Ra_{crit} at different ℓ values, the Rayleigh numbers only have meaning at the integer values of ℓ.

Fig. 1, Cap. on p. 35.

For a particular lithosphere thickness model convection in the mantle sets in when Ra exceeds the minimum of the values of Ra_{crit} shown in Figure 1; the meridional pattern of the convection, at the onset of convection, is determined by that value of ℓ associated with the minimum Ra_{crit}. The minimum values of Ra_{crit} for the thin and thick lithosphere models are

7078.55 and 3177.43, respectively, both associated with the $\ell = 2$ mode of convection. The viscosities associated with the onset of convection are 5.66×10^{23} cm^2/sec and 2×10^{22} cm^2/sec, respectively. In the following, Ra_{crit} will be understood to be the minimum value of the critical Rayleigh numbers.

Lunar Temperature Profiles for Assumed Values of Viscosity

The numerical convection calculations were started using velocity and temperature values from the linearized stability computations for the $\ell = 3$ mode of convection as inputs to the finite-amplitude convection program. An $\ell = 3$, rather than an $\ell = 2$, starting mode was used since the equations of motion do not generate odd ℓ modes from a starting convection pattern in which such modes are completely absent. The convection computations included all modes with $\ell = 1, 2, 3, \ldots\ldots, 16$. Computational times were generally about a thermal diffusion time based on the thickness of the mantle, i.e. $(R_o - R_i)^2/\kappa$. In every case the time of a computation was sufficiently long to establish either a steady-state or, as was more often the situation, a quasi-steady state (see discussion below) in the average temperature.

Steady-state convection was only achieved (within the limitations of the computational time) at low values of the Rayleigh number. Among the results reported here, only the cases $Ra = 10\ Ra_{crit}$ for the thin lithosphere model and

$Ra = 2.5\ Ra_{crit}$ for the thick lithosphere model reached steady-state. In all other cases, i.e. those at higher Rayleigh number, the convection was oscillatory. However, the temperatur averaged over a spherical surface, $T_a(r)$, was remarkably steady compared to the velocity field and the angular dependent components of the temperature field. Fluctuations in $T_a(r)$ were never larger than a few percent; the average temperature profile $T_a(r)$ appears to be a quasi-steady feature of the non-steady convection we find occurring in the internally heated mantle at high Rayleigh numbers!

Generally speaking, there is no single mode which dominates the convection; the first several modes contribute about equally and the contributions of the modes with higher values of ℓ eventually become unimportant for ℓ sufficiently large. Just how large ℓ needs to be to adequately characterize the convection, i.e. how many modes need be retained in the calculation, is a function of the Rayleigh number. The higher Ra, the larger the number of modes required to represent the convection. The sixteen modes we have retained are quite sufficient except perhaps for the largest Rayleigh number, 500 times Ra_{crit}, investigated in the thin lithosphere model.

Fig. 2. Cap. on p. 35.

Figure 2 shows the average (over a spherical surface) lunar temperature as a function of depth in the thin lithosphere model for Rayleigh numbers of 10, 50, 100 and 500 times the critical value, or for viscosities of 10^{-1}, 2×10^{-2}, 10^{-2}, 2×10^{-3} times the value 5.7×10^{23} cm^2/sec (solid lines). Average

temperature profiles of the thick lithosphere model for Ra equal to 1, 2.5, 10 and 50 times Ra_{crit}, or for ν equal to 1, 0.4, 0.1 and 0.02 times 2×10^{22} cm^2/sec are also shown in the figure (dashed lines). With increasing Rayleigh number or decreasing viscosity, there is a decrease in mantle temperature as subsolidus creep becomes a more efficient cooling mechanism. The mantle temperature is rather uniform, especially so at the lower viscosity values. The average temperature profile in the rigid lithosphere is fixed at the solution to the steady-state thermal conduction equation. Although temperatures in the outer part of the thick lithosphere model Moon are smaller than those in the outer part of the thin lithosphere model Moon, the deep temperatures (depth >1000 km) in both models are comparable.

Which of the above profiles (if any) represents the state of the lunar interior depends on rheological considerations to be discussed in the following sections.

SUBSOLIDUS CREEP OF GEOLOGIC MATERIAL

Theoretical models of creep (Weertman 1970) at subsolidus temperatures and at pressures comparable to those in the Earth's upper mantle and throughout the Moon lead to a rheological or constitutive equation of the form

$$\dot{\epsilon} = \left(\frac{B}{T}\right)\exp\left[-\left(E^{*}+pV^{*}\right)/(RT)\right]\tau^{n} \qquad (19)$$

where $\dot{\epsilon}$ is the rate of strain, T is the absolute temperature, p is the pressure, τ is the shear stress and R is the gas constant. The parameter n depends on the microscopic mechanism of deformation, diffusion creep (n = 1) or the motion of dislocations (n > 1), as does the constant B. The activation energy E^{*} and activation volume V^{*} are determined by the diffusion of the slowest, and thus rate-controlling, atomic species. Diffusion creep (Nabarro 1948, Herring 1950) probably applies at low values of stress τ while the mechanism of dislocation motion assumes importance at higher values of stress (Weertman 1970). The value of stress above and below which the different deformation mechanisms become dominant is uncertain and may not even be capable of precise definition; one may speculate that it is $\lesssim$1 bar (see discussion below).

Creep and relaxation experiments (Carter and Avé Lallemand 1970, Post 1973) on olivine yield results in agreement with the above expression, although the 1/T factor in front of the

exponential is usually not resolved and the range of applied pressure is too limited to allow a determination of the pressure dependence. Such measurements and optical or electron transmission microscopy studies of both mantle derived and laboratory deformed olivine crystals (Raleigh 1968, Phakey et al. 1972, Goetze and Kohlstedt 1973) have led to the recognition of the importance of dislocation motion as a mechanism for mantle deformation. Recent analysis by Post and Griggs (1973) of Fennoscandian uplift data suggest a non-Newtonian rheology for the Earth's mantle with $n \approx 3$.

The kinematic viscosity ν is $\tau/(2\rho\dot{\epsilon})$. Using (19) we find

$$\nu = \frac{T}{2\rho B}\tau^{1-n}\exp\left(\frac{E^* + pV^*}{RT}\right) \qquad (20)$$

Except for the Newtonian case ($n = 1$), the viscosity is stress-dependent.

We consider two sets of values for the rheological parameters, a Newtonian one ($n = 1$) and a non-Newtonian one with $n = 3$. For the non-Newtonian case, the values of E^* and B are based on the high-temperature, low-stress (50-1500 bars) creep data of Kohlstedt and Goetze (1974) for dry olivine single crystals. It is important to use values of E^* and B appropriate to dry olivine since the presence of water can drastically alter the rheological parameters of a mineral (Griggs 1974) and the Moon is severely depleted in volatiles (Gast 1972, Kaula 1972). The appropriate values of E^* and B for the non-Newtonian case are

125 kcal/mole and 6.5×10^{-13} cm^3 sec^5 $^\circ K$ gm^{-3}, respectively. The value of V^* probably lies between 10 and 40 cm^3/mole, with the smaller values more likely to be preferable. This uncertainty is not a serious matter since at the pressures in the lunar interior, E^* is an order of magnitude larger than pV^*. We assume $V^* = 11$ cm^3/mole and $p = 35$ kbar, the pressure at a depth of half the lunar radius.

Fig. 3, Cap. on p. 35-36.

The bottom solid curve in Figure 3 shows the ν-T relation for the non-Newtonian case just discussed and an assumed stress $\tau = 1$ bar. The stress level in the interior of the Moon is unknown. Presumably the shear stresses in a convecting lunar mantle would be much less than the stress differences in the lithosphere associated with the mascons. Such stress differences are about 50-100 bars (Kaula 1972, Arkani-Hamed 1973). Since $\nu \propto \tau^{-2}$, $\tau = 10$ bars would result in lunar mantle viscosities much lower than that of the Earth's mantle for which $\nu \approx 10^{22}$ cm^2/sec (Cathles 1971). The upper dashed curve of Figure 3 shows the non-Newtonian effective viscosity for $\tau = 0.1$ bar. At such small τ, the relevant deformation mechanism is probably diffusion creep, in which case the viscosity would be much lower for a given T and the middle solid curve for the diffusion creep or Newtonian viscosity (see below) would be pertinent.

There are no laboratory data demonstrating the Newtonian creep of geologic material. We base our Newtonian viscosity

curve on the equation proposed by Turcotte and Oxburgh (1972) for the viscosity of the Earth's upper mantle (with p = 35 kbar)

$$\nu = \frac{T}{1.21\times10^{-3}}\exp\left(\frac{5.605\times10^{4}}{T}\right) \qquad (21)$$

where T is in °K and ν has units cm^2/sec. It can be seen from Figure 3 that this Newtonian viscosity is very similar in its magnitude and temperature dependence to the effective viscosity of dry olivine undergoing non-Newtonian creep at τ = 1 bar.

We expect either of these ν-T curves to be reasonable representations of the temperature-dependent effective viscosity of the lunar interior.

LUNAR TEMPERATURE: SIMULTANEOUS CONSIDERATION OF CONVECTION CALCULATIONS AND CREEP BEHAVIOR

The temperature profiles of Figure 2 show that the spherically-averaged temperature of the lunar mantle is nearly constant, especially at the higher Rayleigh numbers or lower viscosities. Thus we can associate a single temperature, e.g. the mean temperature of the lower 3/4 of the lunar mantle (by radius), with convection at a particular Rayleigh number or mantle viscosity. We show these convection temperatures as functions of viscosity by the shaded bands on Figure 3, the upper band for the thin lithosphere model and the lower one for the thick lithosphere model. The thickness of the bands represents our estimate of the uncertainty in the convection temperature for a given viscosity. The uncertainty estimate includes the fact that there are temperature variations in the mantle, especially near the mantle-lithosphere interface. Perhaps more importantly, the uncertainty takes into account the fluctuations of a few percent in the numerical calculations of the average temperature (recall the quasi-steady nature of the average convection temperatures at the higher Rayleigh numbers).

Since the temperature and viscosity in the lunar mantle must self-adjust to satisfy the constraints of the deformation

law and the convection calculations, the intersections of the shaded regions with either of the solid curves in Figure 3 simultaneously determine the mantle temperatures and viscosities of thin and thick lithosphere models. For either model, the average mantle temperature is between about 1550 °K and 1620 °K and the average mantle viscosity lies between 10^{21} cm^2/sec and $5x10^{21}$ cm^2/sec. Considering the uncertainties in the creep behavior of the material and the approximate nature of the convection calculations, conservative estimates of the temperature and viscosity of the lunar mantle are 1500-1600 °K and 10^{21}-10^{22} cm^2/sec, respectively.

It is noteworthy that the thermal and viscous states of the mantle of both the thin and thick lithosphere models are essentially the same. Thus our computation of the deep lunar temperature is quite insensitive to the assumed lithosphere thickness, provided the radiogenic heat source concentration is 'consistent' (from the steady state point of view) with this thickness. Of course, this conclusion cannot be carried to the extreme wherein the depletion of radioactives from the interior of the Moon is so large as to preclude convection from occurring at all.

There is essentially no difference in the thermal and mechanical states of the very deep interiors of the thin and thick lithosphere model Moons (as can be seen in Figures 2 and 3). The thin lithosphere model has a much more uniform

average temperature throughout the interior, which extends to within about 500 km of the surface. The thick lithosphere model has, of course, much lower temperatures in the outer 1000 km of the Moon with the temperature rising essentially along a conduction profile and levelling out at the uniform mantle temperature at a depth of about 1000 km.

If the thickness of the Moon's lithosphere is 300 km or less, then geologic time is sufficient for the establishment of a steady conduction temperature in the rigid lithosphere; for the mantle, we have noted that quasi-steady average temperatures are established in a region of convection on a time scale of only 0.1 the conduction time for the region. If the lithosphere is indeed as thick as 800 km then it is possible that a steady thermal state has not been established in either the lithosphere or mantle.

CONCLUSIONS: COMPARISON OF THERMAL MODELS WITH INFERENCES FROM GEOPHYSICAL DATA

Lunar Heat Flux Measurements

In situ lunar surface heat flow determinations are 0.74 $\mu cal/cm^2$ sec at the Apollo 15 site, and 0.67 $\mu cal/cm^2$ sec for one probe location and 0.60 $\mu cal/cm^2$ sec for a second probe location at the Apollo 17 site (Langseth et al. 1973). If these lunar heat flux values are representative of the global average, and if the lunar and terrestrial heat flows measure the total amount of internal radioactive heat generation in the respective bodies, then the average lunar concentration of radiogenic sources is about 2.5 times as large as the terrestrial one. Clearly there has been an upward concentration of radioactivity on the Moon associated with the differentiation of at least the outer several hundred kilometers of the body. Thus we cannot infer the value of the deep radiogenic source concentration from the surface heat flux measurements. Remote and terrestrial-based observations of the lunar microwave emission spectrum give hope of eventually providing a global average lunar surface heat flux (Keihm and Langseth 1975).

Seismic Observations

Lunar seismic data from distant meteroid impacts, high frequency teleseismic events and deep moonquakes have led Nakamura et al. (1974) to conclude that there exists a zone of high shear wave attenuation below a depth of about 800 km (see also Nakamura et al. 1973) and that there may exist a zone of radius 170 to 360 km at the center of the Moon characterized by a greatly reduced P-wave velocity. They speculate that partial melting may occur in the region of shear wave attenuation and that a small molten core of iron sulphide may exist. In addition, the P and S wave velocities at depths of several hundred kilometers are consistent with a mineral assemblage of olivine and pyroxene (see also Duba and Ringwood 1973) which is richer in the former mineral.

The deep lunar temperature we calculate here, 1500-1600 °K, is sufficiently high that it may correspond, or approach very closely, to lunar solidus temperatures at depths greater than about 800 km. Our estimate of the deep temperature is about 300 °K lower than the melting point of iron at pressures above about 40 kbars (Higgins and Kennedy 1971). Therefore it is consistent only with a solid pure iron core or a molten Fe core with a light alloying element which depresses the melting point.

Electrical Conductivity Determinations

Electrical conductivity profiles of the Moon, inferred from simultaneous surface and orbiter magnetic measurements, together with laboratory data on the electrical conductivity of olivines and pyroxenes as functions of temperature and oxygen fugacity, provide estimates of the deep lunar temperature. Duba and Ringwood (1973) have used data on the electrical conductivity of these minerals at oxygen fugacities supposedly characteristic of the lunar interior and electrical conductivity models of Sonett et al. (1971) to infer deep lunar temperatures in the range 1550-1750 °K. These temperatures are in excellent agreement with the temperatures 1500-1600 °K of the solid state convection thermal models of this paper.

An important aspect of the lunar electrical conductivity models (Sonett et al. 1972) is that below about 200 km depth the conductivity rises only very slowly with depth, indicative of a nearly uniform temperature as would result from heat transport by subsolidus creep (Turcotte et al. 1972, Kuckes 1972). This characteristic of the lunar electrical conductivity provides support for the thin lithosphere model of this paper (thickness $\lesssim$300 km), wherein much of the Moon's interior is at a nearly uniform temperature maintained by solid state convective cooling.

ACKNOWLEDGMENT

This work was supported in part by NASA under NGL 05-007-002.

REFERENCES

Arkani-Hamed, J. 1973 On the thermal history of the moon. The Moon 6, 380-383.

Carter, N. L. and H. G. Avé Lallemand 1970 High temperature flow of dunite and peridotite. Geol. Soc. of Am. Bull. 81, 2181-2202.

Cassen, P. and R. T. Reynolds 1973 The role of convection in the moon. J. Geophys. Res. 78, 3203-3215.

Cassen, P. and R. T. Reynolds 1974 Convection in the moon: Effect of variable viscosity. J. Geophys. Res. 79, 2937-2944.

Cassen, P. and R. E. Young 1975 On the cooling of the moon by solid convection. The Moon, in press.

Cathles, L. M., III 1971 Lower mantle viscosity inferred from postglacial adjustment of the ocean basins and Canada. EOS Trans. AGU 52, 353.

Chandrasekkar, S. 1961 Hydrodynamic and Hydromagnetic Stability. Oxford: Clarendon Press.

Duba, A. and A. E. Ringwood 1973 Electrical conductivity, internal temperatures and thermal evolution of the moon. The Moon 7, 356-376.

Ganguly, J. and G. C. Kennedy 1975 Solubility of K in Fe-S liquid, silicate-K-$(Fe\text{-}S)^{liq}$ equilibria, and their planetary implications. J. Geophys. Res., submitted to.

Gast, P. W. 1972 The chemical composition and structure of the moon. The Moon 5, 121-148.

Goetze, C. and D. L. Kohlstedt 1973 Laboratory study of dislocation climb and diffusion in olivine. J. Geophys. Res. 78, 5961-5971.

Griggs, D. T. 1974 A model of hydrolytic weakening of quartz. J. Geophys. Res. 79, 1653-1661.

Herring, C. 1950 Diffusional viscosity of a polycrystalline solid. J. Appl. Phys. 21, 437-445.

Higgins, G. and G. C. Kennedy 1971 The adiabatic gradient and the melting point gradient in the core of the earth. J. Geophys. Res. 76, 1870-1878.

Kaula, W. M. 1972 Physical structure of the moon. Proc. Int. Geol. Cong. 15, 35-39.

Kaula, W. M., G. Schubert, R. E. Lingenfelter, W. L. Sjogren and W. R. Wollenhaupt 1974 Apollo laser altimetry and inferences as to lunar structure. Proc. Fifth Lunar Science Conf., Vol. 3 (3049-3058). New York: Pergamon Press.

Keihm, S. J. and M. G. Langseth 1975 Microwave emission spectrum of the moon: Mean global heat flow and average depth of the regolith. Science 187, 64-66.

Kohlstedt, D. L. and C. Goetze 1974 Low-stress and high-temperature creep in olivine single crystals. J. Geophys. Res. 79, 2045-2051.

Kuckes, A. F. 1974 Lunar magnetometry and mantle convection. Nature 252, 670-672.

Langseth, M. G., Jr., S. J. Keihm and J. L. Chute, Jr. 1973 Heat flow experiment. Apollo 17 Preliminary Science Report, NASA SP-330. Washington, D. C.: U. S. Gov't. Printing Office.

Meissner, R. 1975 Lunar viscosity as obtained from the selenotherms. The Moon 12, 179-191.

Nabarro, F. R. N. 1948 Deformation of crystals by the motion of single ions. Conference on the Strength of Solids (75-90). London: The Physical Society.

Nakamura, Y., D. Lammlein, G. Latham, M. Ewing, J. Dorman, F. Press and N. Toksöz 1973 New seismic data on the state of the deep lunar interior. Science 181, 49-51.

Nakamura, Y., G. Latham, D. Lammlein, M. Ewing, F. Duennebier and J. Dorman 1974 Deep lunar interior inferred from recent seismic data. Geophys. Res. Lett. 1, 137-140.

Phakey, P., G. Dollinger and J. Christie 1972 Transmission electron microscopy of experimentally deformed olivine crystals. Flow and Fracture of Rocks (eds. H. C. Heard, I. Y. Borg, N. L. Carter, C. B. Raleigh, Geophys. Monograph 16) (117-138). Washington, D. C.: American Geophysical Union.

Post, R. L. 1973 The flow laws of Mount Burnett dunite. Ph.D. Thesis, University of California, Los Angeles.

Post, R. L. and D. T. Griggs 1973 The earth's mantle: Evidence of non-newtonian flow. Science 181, 1242-1249.

Raleigh, C. B. 1968 Mechanisms of plastic deformation in olivine. J. Geophys. Res. 73, 5391-5406.

Runcorn, S. K. 1962 Convection in the moon. Nature 195, 1150-1151.

Runcorn, S. K. 1967 Convection in the moon and the existence of a lunar core. Proc. Roy. Soc., Ser. A. 296, 270-284.

Schubert, G., D. L. Turcotte and E. R. Oxburgh 1969 Stability of planetary interiors. Geophys. J. Roy. Astr. Soc. 18, 441-460.

Sjogren, W. L. 1971 Lunar gravity estimate: Independent confirmation. J. Geophys. Res. 76, 7021-7026.

Sonett, C. P., D. S. Colburn, P. Dyal, C. W. Parkin, B. F. Smith, G. Schubert and K. Schwartz 1971 The lunar electrical conductivity profile. Nature 230, 359-362.

Sonett, C. P., B. F. Smith, D. S. Colburn, G. Schubert and K. Schwartz 1972 The induced magnetic field of the moon: Conductivity profiles and inferred temperature. Proc. Third Lunar Science Conf., Vol. 3 (2309-2336). Cambridge: The M.I.T. Press.

Turcotte, D. L. and E. R. Oxburgh 1972 Mantle convection and the new global tectonics. Annual Rev. of Fluid Mech. 4, 33-68.

Turcotte, D. L., A. T. Hsui, K. E. Torrance and E. R. Oxburgh 1972 Thermal structure of the moon. J. Geophys. Res. 77, 6931-6939.

Weertman, J. 1970 The creep strength of the earth's mantle. Rev. of Geophys. and Space Phys. 8, 145-168.

Williams, J. G., W. S. Sinclair, M. A. Slade, P. L. Bender, J. P. Hauser, J. D. Mulholland and P. J. Shelus 1974 Lunar moment of inertia constraints from lunar lasor ranging. Lunar Science V (845). Houston: The Lunar Science Institute.

Young, R. E. 1974 Finite amplitude thermal convection in a spherical shell. J. Fluid Mech. 63, 695-721.

FIGURE CAPTIONS

Figure 1. Critical Rayleigh numbers Ra_{crit} for the onset of convection (according to linearized stability theory) in internally heated models of the lunar mantle as a function of the spatial pattern at the onset of convection, given by the degree ℓ of the associated Legendre function $P_\ell(\cos\theta)$ (θ is the colatitude). Only the values of Ra_{crit} at integer values of ℓ are significant.

Figure 2. Models of the average (over a spherical surface) temperature of the Moon as a function of depth, based on numerical, finite-amplitude calculations of convection in a lunar mantle with constant viscosity and a uniform concentration of radioactive heat sources. The solid curves refer to a Moon model with a 300 km thick rigid lithosphere and a terrestrial concentration of heat sources; the model associated with the dashed curves has an 800 km thick lithosphere and 50% of the terrestrial heat source concentration. The numbers associated with each temperature profile are the Rayleigh number (in terms of Ra_{crit} for each model) and the mantle viscosity, respectively.

Figure 3. Viscosity-temperature relations based on the creep behavior of geologic material and the numerical calculations of convection in the Moon's interior. The bottom

solid line gives the effective viscosity of dry olivine undergoing non-Newtonian deformation at a shear stress of 1 bar; the upper dashed line is a similar viscosity curve for a shear stress of 0.1 bar. The middle solid line is a viscosity associated with Newtonian or diffusion creep. The upper shaded band gives the average mantle convection temperature for the model with a 300 km thick lithosphere; the lower band provides the same temperatures for the 800 km thick lithosphere model. The widths of the bands approximate the uncertainties in the calculated mantle temperatures. The intersections of the bands with either of the solid curves yield estimates of the deep lunar temperature and associated viscosity.

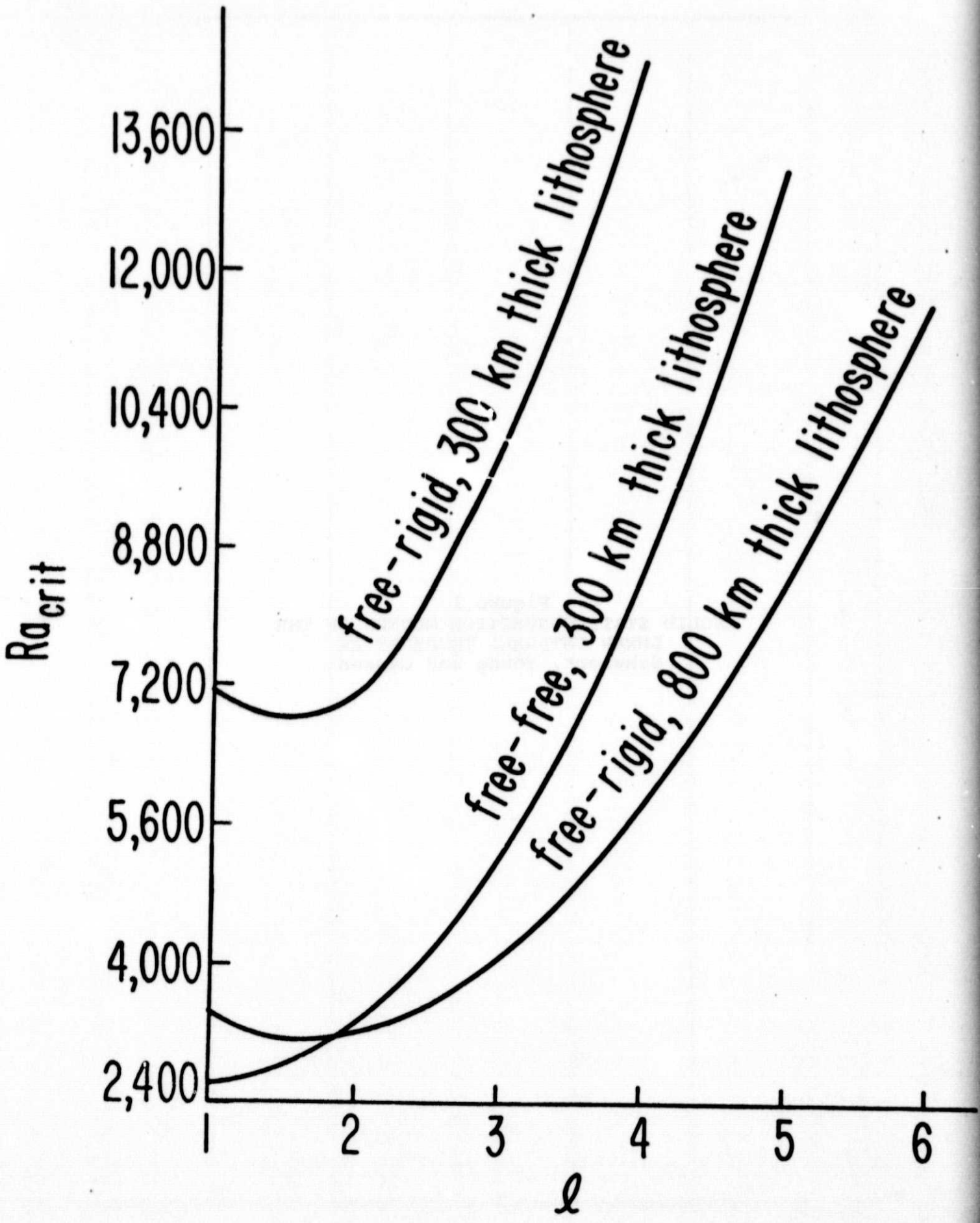
13,600
12,000
10,400
8,800
7,200
5,600
4,000
2,400
Ra crit
1
2
3
4
5
6
ℓ
free-rigid, 300 km thick lithosphere
free-free, 300 km thick lithosphere
free-rigid, 800 km thick lithosphere

Fig. 1

Figure 1
SOLID STATE CONVECTION MODELS OF THE
LUNAR INTERNAL TEMPERATURE
Schubert, Young and Cassen

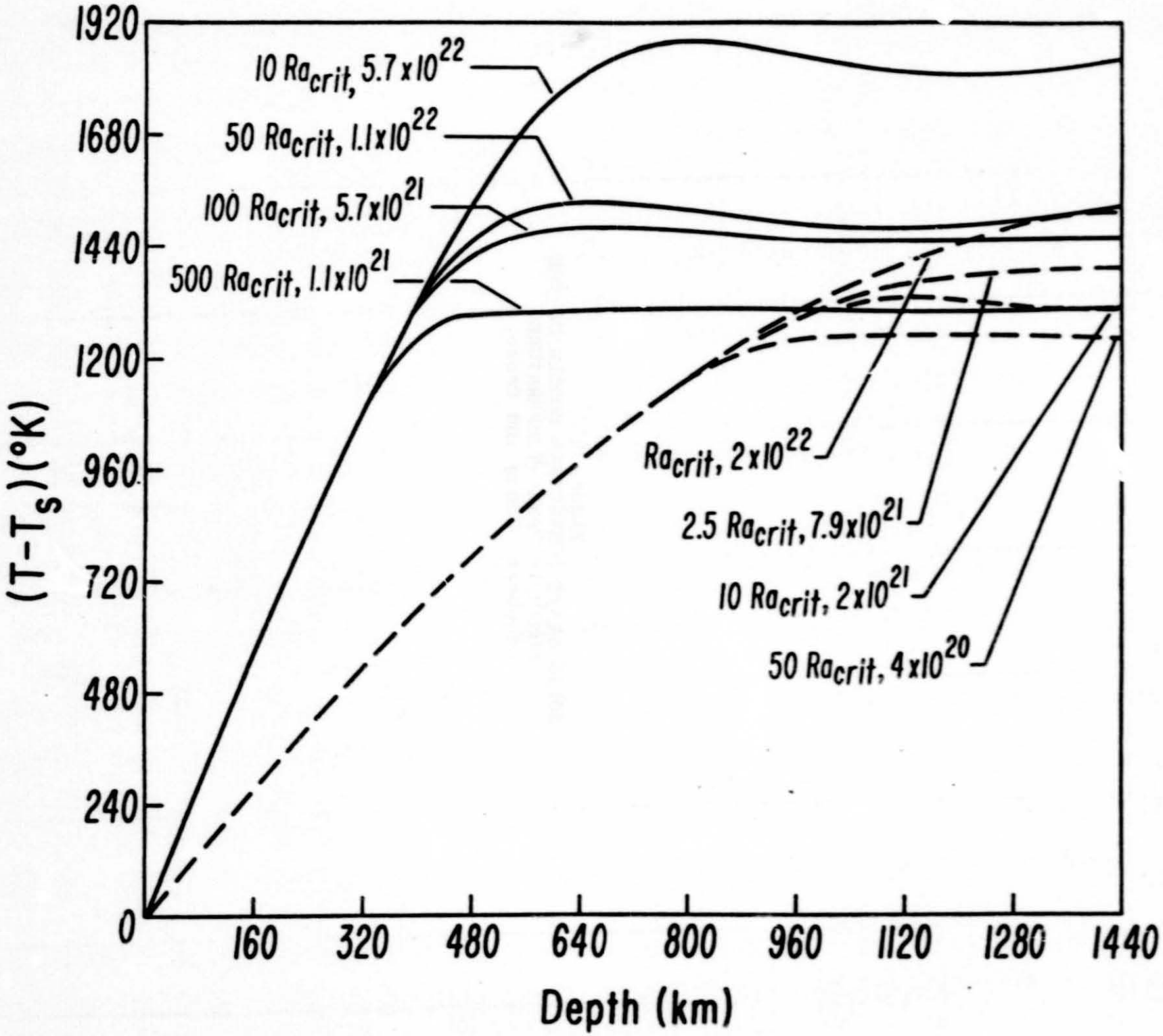
1920
1680
1440
1200
960
720
480
240
0
160
320
480
640
800
960
1120
1280
1440
Depth (km)
(T-T_S)(°K)
10 Ra_crit, 5.7x10^22
50 Ra_crit, 1.1x10^22
100 Ra_crit, 5.7x10^21
500 Ra_crit, 1.1x10^21
Ra_crit, 2x10^22
2.5 Ra_crit, 7.9x10^21
10 Ra_crit, 2x10^21
50 Ra_crit, 4x10^20

Fig. 2

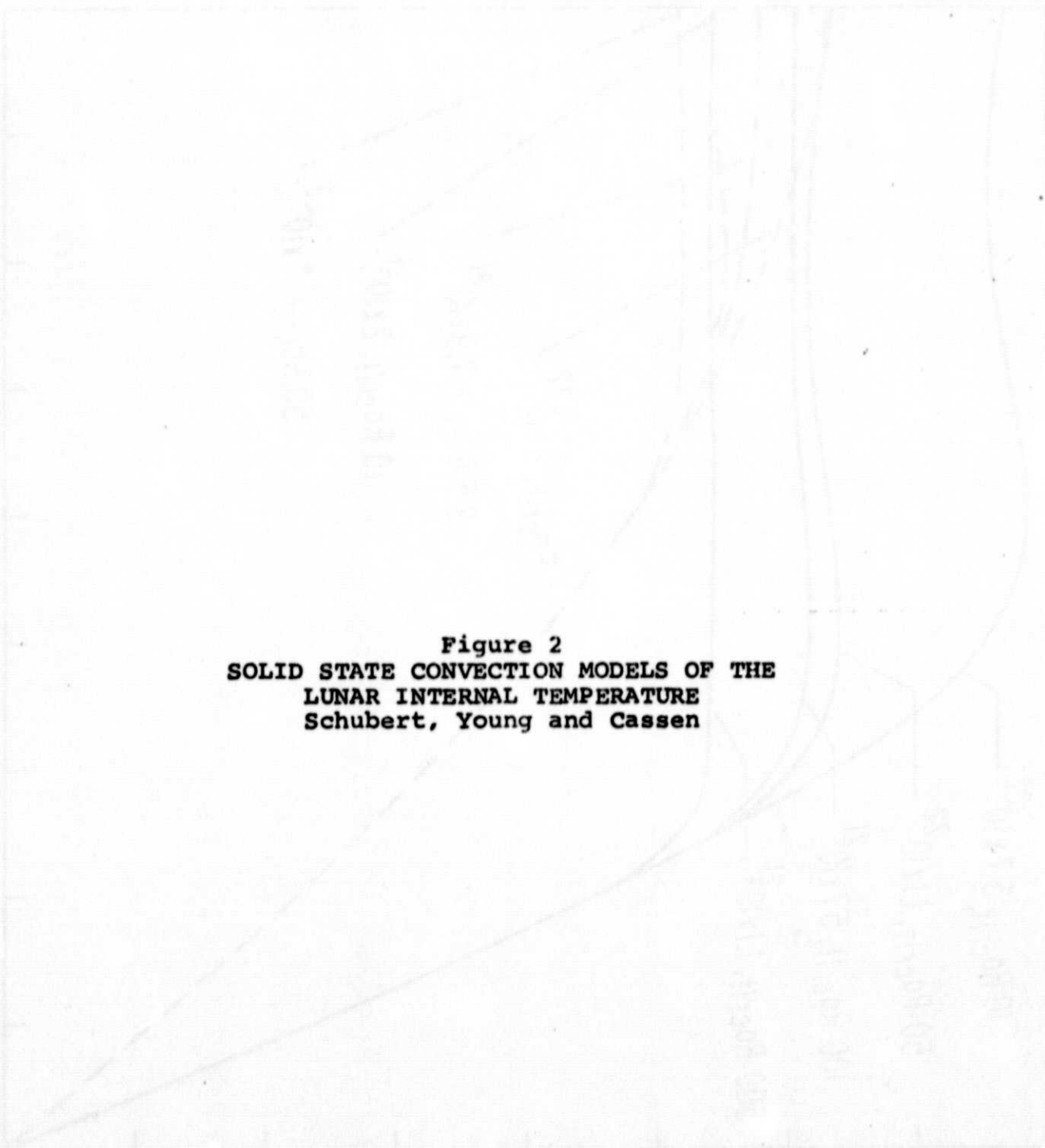

Figure 2
SOLID STATE CONVECTION MODELS OF THE
LUNAR INTERNAL TEMPERATURE
Schubert, Young and Cassen

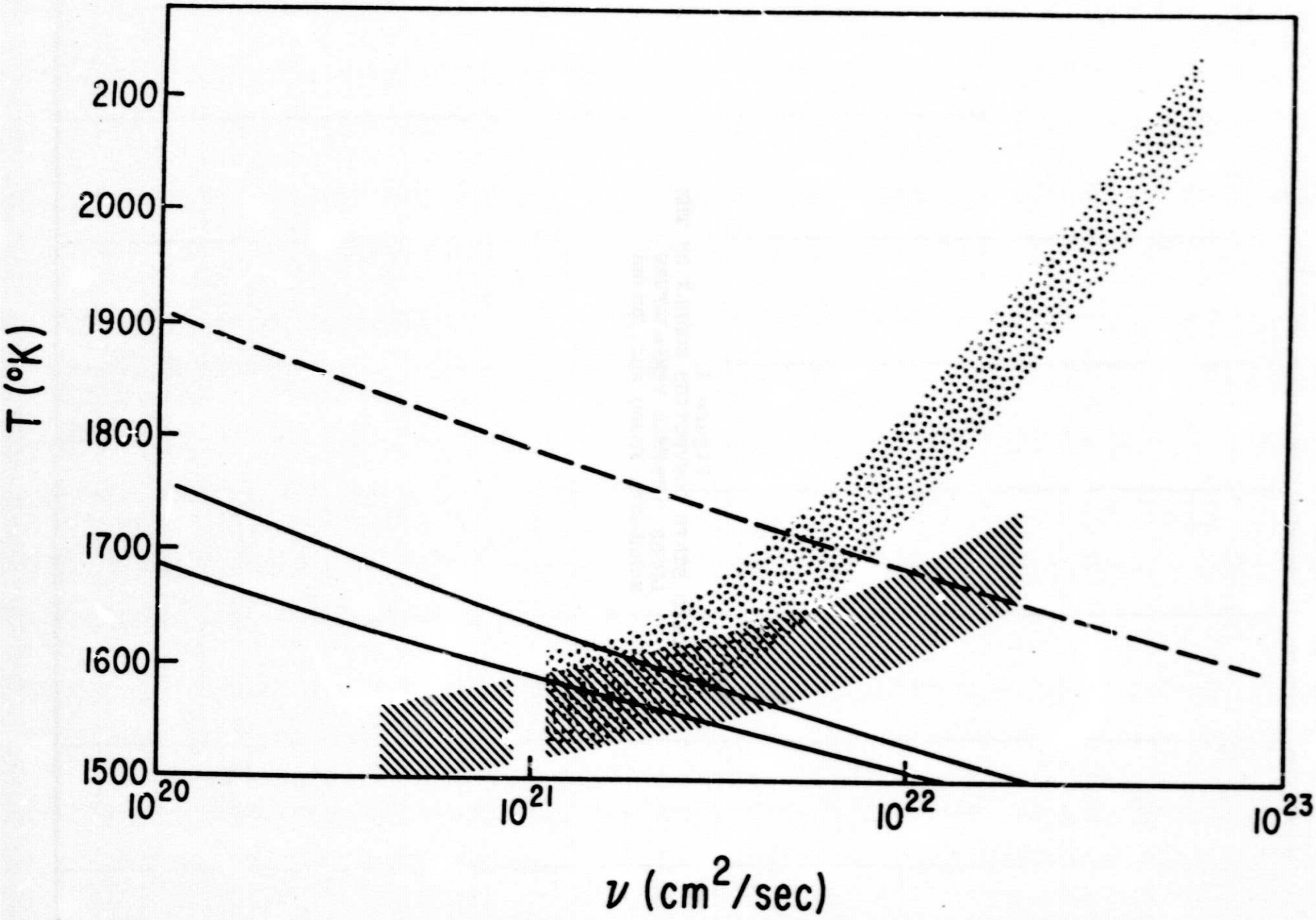
2100
2000
1900
1800
1700
1600
1500
T (°K)
10^{20}
10^{21}
10^{22}
10^{23}
ν (cm^2/sec)

Fig. 3

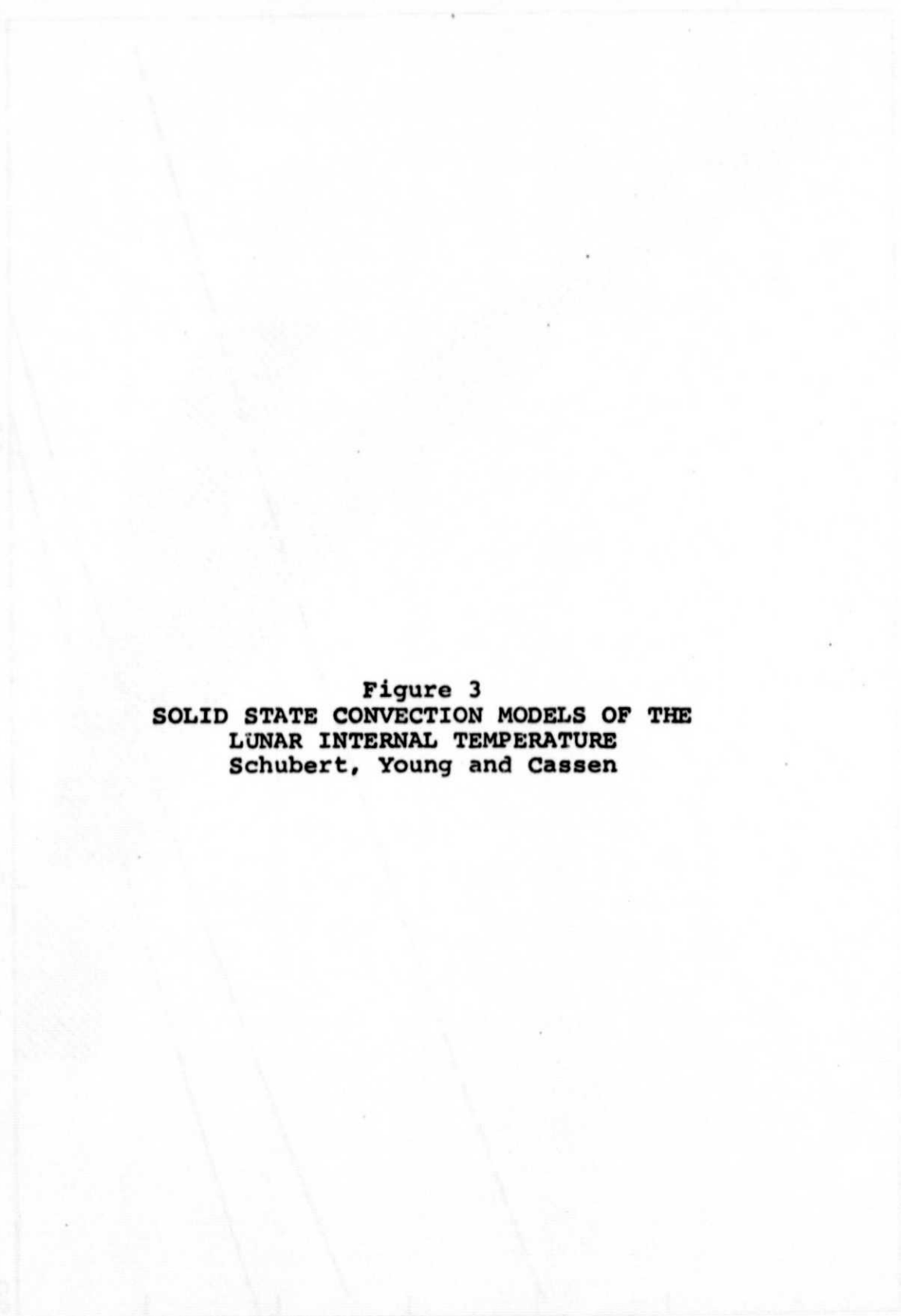

Figure 3
SOLID STATE CONVECTION MODELS OF THE
LUNAR INTERNAL TEMPERATURE
Schubert, Young and Cassen